TRANSIENT RESPONSE DYNAMIC MODULE MODIFICATIONS TO INCLUDE STATIC AND KINETIC FRICTION EFFECTS

J. E. Misel*, S. B. Nenno*, and D. Takahashi*
Shuttle Integration and Satellite Systems Division
Rockwell International

SUMMARY

A methodology that supports forced transient response dynamic solutions when both static and kinetic friction effects are included in a structural system model is described herein. Modifications that support this type of nonlinear transient response solution are summarized for the transient response dynamics (TRD) NASTRAN module. An overview of specific modifications for the NASTRAN processing subroutines, INITL, TRD1C, and TRD1D, are described with further details regarding inspection of nonlinear input definitions to define the type of nonlinear solution required, along with additional initialization requirements and specific calculation subroutines to successfully solve the transient response problem.

The extension of the basic NASTRAN nonlinear methodology is presented through several stages of development to the point where constraint equations and residual flexibility effects are introduced into the finite difference Newmark-Beta recurrsion formulas. Particular emphasis is placed on cost effective solutions for large finite element models such as the Space Shuttle with friction degrees of freedom between the orbiter and payloads mounted in the cargo bay. An alteration to the dynamic finite difference equations of motion is discussed, which allows one to include friction effects at reasonable cost for large structural systems such as the Space Shuttle. Also presented is an hypothesis that suggests that a correlation exists between flexibility loss data at the friction degrees of freedom and solution accuracy when truncated modal coordinates are employed in the equations of motion for a structural system. A friction demonstration problem is included to show how residual flexibilities dramatically improve the solution accuracy of the forced dynamic response when truncated modal coordinates are implemented for the structural response problem. The residual flexibility correction effects may be applied to other nonlinear transient response problems not considered in this paper. The numerical results of the idealized and highly simplified structural transient response problem also demonstrates the completeness of the approach by providing the capability to obtain nonlinear response solutions when either physical or modal coordinates are used.

Finally, data are presented to indicate the possible impact of transient friction loads to the payload designer for the Space Shuttle. Transient response solution data are also included, which compare solutions without friction forces and those with friction forces for payloads mounted in the Space Shuttle cargo bay. These data indicate that payload components can be sensitive to friction induced loads.

INTRODUCTION

The Space Shuttle has been designed to carry a large class of payloads to low earth orbit (LEO). The standard structural load path between the orbiter and the payload is a set of trunnions. A longeron trunnion is illustrated in figure 1. This system of attaching payloads offers much flexibility in the types, sizes, locations in the orbiter cargo bay, and mixes of payloads that can be integrated into the Space Shuttle.

The trunnion restraint system allows relative motion between the orbiter and the payload in the axial direction of the trunnion, as shown in figure 1. Relative motion can also be accommodated in the orbiter longitudinal direction. The relative motions are necessary to preclude large thermally induced loads between the orbiter and the payload during on-orbit mission operations and reentry; however, transient relative motion will be experienced during dynamic events, and the resulting transient friction loads acting on the trunnion may be a factor for the payload system structural design.

As a result of these inherent design features, the effects of trunnion friction on Space Shuttle payload transient loads have become a concern to various payload organizations. Friction behavior at the interface between payloads and the orbiter or within the payload system imposes nonlinear responses on the payload that are not generally included in payload

*Member of the Technical Staff

linear load analysis. These nonlinearities associated with friction forces can significantly affect dynamic responses, which, in turn, will impact certain payload design parameters. Nonlinear friction characteristics such as these have been investigated for satellites cantilevered to the inertial upper stage (IUS).

Various methodologies have been developed recently to perform loads analyses with interface friction forces included for Shuttle payloads. These methodologies have resulted in differing payload responses, that are apparently caused by different approximations. Because of the importance to the payload structural design, it is imperative that the nonlinear friction methodology accurately reflect all aspects of the friction phenomenon. Thus, this new analysis procedure that has been developed, and as described here, addresses both types of friction effects: kinetic (or sliding friction), and static friction (or stiction), which exhibits a nonuniform friction coefficient as forces change.

As friction surfaces lock and unlock, the system modal characteristics also change. Modal data are considered for two primary reasons. First, the large size of the orbiter and payload finite element structural models prohibit the use of direct solutions without the sophistication of modal coordinate transformations. Secondly, modal data are generally employed in analyzing large finite element structural models for linear transient loads analyses. For a system with N friction surfaces, 2^N different sets of modal data are possible. The 2^N possible sets of modes are accounted for in the approach described later by including N constraint equations in the system equations of motion. The constraining equations are imposed on the system equations of motion according to program solution logic that enforces stiction or sliding friction as required throughout the transient response solution. As a result, the accuracy of the relative displacement terms associated with the interface compatibility constraint relations must be enhanced by the use of residual flexibilities. The nonlinear capabilities of NASTRAN have been expanded to include both kinetic and static friction conditions in Space Shuttle payload transient loads analysis.

NASTRAN NONLINEAR METHODOLOGY

The equations representing the dynamic behavior of a structure may be written in matrix form as

$$[M]\{\ddot{u}\} + [B]\{\dot{u}\} + [K]\{u\} = \{F\} \tag{1}$$

Reduction of solution costs are usually accomplished through transformation to a set of uncoupled modal coordinates followed by truncation of higher frequency modes. This approximation is generally sufficient to represent a system whose response is primarily confined to the lower frequency regions. After substitution of the normal coordinate transformation, the equations of motion in modal coordinates are

$$[I]\{\ddot{q}\} + 2[\zeta\omega]\{\dot{q}\} + [\omega^2]\{q\} = [\Phi]^T\{F\} = \{\bar{P}\} \tag{2}$$

Equation (2) was obtained from the relation

$$\{u\} = [\Phi]\{q\} \tag{3}$$

The inclusion of nonlinear effects into a linear structural system can be accomplished by employing NASTRAN's standard nonlinear capability. This involves treating nonlinearities as a combination of calculated nonlinear loads, which are added to the external load vector, and a set of auxiliary equations used in the calculation of these nonlinear loads that is appended to the linear equations of motion. The auxiliary equations are defined using the NASTRAN extra point and DMIG features. The resulting system of equations is

$$\begin{bmatrix} I & 0 & 0 \\ A & 0 & 0 \\ 0 & 0 & 0 \end{bmatrix} \begin{Bmatrix} \ddot{q} \\ \ddot{e} \\ \ddot{N} \end{Bmatrix} + \begin{bmatrix} 2\zeta\omega & 0 & 0 \\ C & 0 & 0 \\ 0 & 0 & 0 \end{bmatrix} \begin{Bmatrix} \dot{q} \\ \dot{e} \\ \dot{N} \end{Bmatrix} + \begin{bmatrix} \omega^2 & 0 & F \\ D & I & E \\ 0 & 0 & I \end{bmatrix} \begin{Bmatrix} q \\ e \\ N \end{Bmatrix} = \begin{Bmatrix} \bar{P} \\ 0 \\ \bar{N} \end{Bmatrix} \tag{4}$$

In the above equation, e represents a response vector of velocities, relative displacements, and normal forces that are used in calculating N, the nonlinear forces. These equations may be formulated and solved in any desired system of coordinates by applying the appropriate transformations.

The presence of auxiliary equations in equation (4) results in a coupled system that must be solved using a numerical integration procedure. The method used in NASTRAN is a modified Newmark-Beta scheme. This finite difference algorithm is noniterative and inherently stable. A brief development of the finite difference equations used in the TRD module will be given here. A more rigorous treatment can be found in the NASTRAN theoretical manual (ref. 1). To aid in developing the finite difference equations, equation (4) may be written in symbolic form as

$$[\overline{M}]\{\ddot{\bar{u}}\} + [\overline{B}]\{\dot{\bar{u}}\} + [\overline{K}]\{\bar{u}\} = \{\overline{Q}\} = \{\overline{P}\} + \{\overline{N}\} \tag{5}$$

where $\overline{P}$ represents the linear external forces and $\overline{N}$ represents the nonlinear forces. The finite difference equations used in the integration scheme are as follows

$$\dot{\bar{u}} = 1/2\Delta t(\bar{u}_{n+1} - \bar{u}_{n-1}) \tag{6}$$

$$\ddot{\bar{u}} = 1/\Delta t^2(\bar{u}_{n+1} - 2\bar{u}_n + \bar{u}_{n-1}) \tag{7}$$

$$\bar{u} = 1/3(\bar{u}_{n+1} + \bar{u}_n + \bar{u}_{n-1}) \tag{8}$$

$$\overline{P} = 1/3(\overline{P}_{n+1} + \overline{P}_n + \overline{P}_{n-1}) \tag{9}$$

$$\overline{N} = 1/3(\overline{N}_n + \overline{N}_{n-1} + \overline{N}_{n-2}) \tag{10}$$

Substitution of equations (6) through (10) into equation (5) results in the recursion relation

$$\begin{aligned}(1/\Delta t^2\overline{M} + 1/2\Delta t\overline{B} + 1/3\overline{K})\bar{u}_{n+1} &= 1/3(\overline{P}_{n+1} + \overline{P}_n + \overline{P}_{n-1}) \\ &+ 1/3(\overline{N}_n + \overline{N}_{n-1} + \overline{N}_{n-2}) + (2/\Delta t^2\overline{M} - 1/3\overline{K})\bar{u}_n + \\ &(-1/\Delta t^2\overline{M} + 1/2\Delta t\overline{B} - 1/3\overline{K})\bar{u}_{n-1}\end{aligned} \tag{11}$$

The unknown displacements $\bar{u}_{n+1}$ can then be solved for in terms of previously determined quantities. This equation may be written as

$$\tilde{K}\bar{u}_{n+1} = \tilde{P}_{n+1} \tag{12}$$

where

$$\tilde{K} = 1/\Delta t^2\overline{M} + 1/2\Delta t\overline{B} + 1/3\overline{K} \tag{13}$$

and $\tilde{P}_{n+1}$ is the entire right-hand side of equation (11).

Here, $\tilde{K}$ is constant for constant Δt. By applying this scheme, forces and displacements are assumed to be essentially invariant over the integration step. In order for this assumption to hold, it is imperative that Δt be sufficiently small.

NONLINEAR METHODOLOGY WITH FRICTION FORCES

The inclusion of friction nonlinearities into an analysis presents a problem that cannot be solved using the standard NASTRAN nonlinear methodology just described. This occurs because friction is actually a combination of two complementary phenomena. There is kinetic friction, which is treated as a finite force that opposes the relative motion of two contacting surfaces and static friction.

Kinetic friction is straightforward in nature and may be simulated by using the equation

$$f_k = \mu_k \cdot N \cdot \text{sign}(\Delta\dot{u}_{rel}) \tag{14}$$

In equation (14), f_k is the kinetic friction force, μ is the kinetic coefficient of friction, N is the normal force between the two friction surfaces, and $\Delta\dot{u}_{rel}$ is the relative velocity of the friction surfaces. Kinetic friction is a nonlinearity that is similar in nature to the discrete damper and may thus be analyzed with standard NASTRAN solution procedures.

However, the inclusion of static friction or stiction poses a problem. Static friction exists when the relative velocity of two surfaces tends to zero. Physically, the friction surfaces lock and provide a continuous load path. In effect, the equations of motion experience additional constraint relationships. In order to model this occurrence, a new methodology has been developed and implemented in NASTRAN.

Static friction is modeled by adding a set of constraint equations enforcing a constant relative displacement over the period of integration to equation (11). A set of friction degrees of freedom (DOF) u_I may be defined, with u_D being its complementary set of friction DOF, and u_F being all remaining DOF. Equation (12) may be expanded, using e points, to include the constraint equations between u_I and u_D. The friction model equation then becomes

$$\begin{bmatrix} \bar{K}_{FF} & \bar{K}_{FI} & \bar{K}_{FD} & 0 \\ \bar{K}_{IF} & \bar{K}_{II} & \bar{K}_{ID} & -I \\ \bar{K}_{DF} & \bar{K}_{DI} & \bar{K}_{DD} & -I \\ 0 & -I & -I & 0 \end{bmatrix} \begin{Bmatrix} \bar{u}_F \\ \bar{u}_I \\ \bar{u}_D \\ f_s \end{Bmatrix}_{n+1} = \begin{Bmatrix} \bar{P}_F \\ \bar{P}_I \\ \bar{P}_D \\ q_r \end{Bmatrix}_{n+1} \tag{15}$$

where f_s is the stiction force required to enforce a constant relative displacement q_r. These equations serve to enforce stiction between $\bar{u}_I$ and $\bar{u}_D$. Equation (15) can further be expressed as the following three equations:

$$\begin{bmatrix} \bar{K}_{FF} & \bar{K}_{FI} + \bar{K}_{FD} \\ \bar{K}_{IF} + \bar{K}_{DF} & \bar{K}_{II} + \bar{K}_{DI} + \bar{K}_{ID} + \bar{K}_{DD} \end{bmatrix} \begin{Bmatrix} \bar{u}_F \\ \bar{u}_I \end{Bmatrix}_{n+1} =$$

$$\begin{Bmatrix} \bar{P}_F + \bar{K}_{FD} q_r \\ \bar{P}_I + \bar{P}_D + (\bar{K}_{DD} + \bar{K}_{ID}) q_r \end{Bmatrix}_{n+1} \tag{15a}$$

$$\{\bar{u}_D\}_{n+1} = \{\bar{u}\}_{n+1} - \{q_r\}_{n+1} \tag{15b}$$

$$\{f_s\}_{n+1} = \{\bar{P}_I\}_{n+1} - [\bar{K}_{IF}]\{\bar{u}_F\}_{n+1} - [\bar{K}_{II}]\{\bar{u}_I\}_{n+1} - [\bar{K}_{ID}]\{\bar{u}_D\}_{n+1} \tag{15c}$$

The solution of equations (15a) and (15b) yield the displacements u_I and u_D. The static friction force f_s can then be determined from equation (15c). Note that f_s does not appear in equations (15a) or (15b); therefore, it is considered to be an internal load. For the state when all friction surfaces are free to slide (kinetic friction only), the constraint equations in equation (15) are modified and read as

$$\begin{bmatrix} \bar{K}_{FF} & \bar{K}_{FI} & \bar{K}_{FD} & 0 \\ \bar{K}_{IF} & \bar{K}_{II} & \bar{K}_{ID} & -I \\ \bar{K}_{DF} & \bar{K}_{DI} & \bar{K}_{DD} & -I \\ 0 & 0 & 0 & -I \end{bmatrix}_{n+1} \begin{Bmatrix} \bar{u}_F \\ \bar{u}_I \\ \bar{u}_D \\ f_s \end{Bmatrix}_{n+1} = \begin{Bmatrix} \bar{P}_F \\ \bar{P}_I \\ \bar{P}_D \\ f_k \end{Bmatrix}_{n+1} \tag{16}$$

As stated earlier, kinetic and static friction are complementary events and thus equations (15) and (16) may be used to represent any combination of sliding and nonsliding surfaces. In the analysis procedure, f_k is calculated at every time step and compared against f_s, which is computed only during periods of near-zero relative motion. The kinetic and static friction forces are then compared and the appropriate constraint equations are applied. This set of constraint equations

defines the friction state of the structure. For a structure having N friction surfaces, there are 2^N possible friction states. Finally, the actual friction force at any instant of time is chosen to be either the kinetic or static friction force.

This presentation indicates that the friction solution is dependent on a set of calculated displacements. As a result, the displacement field representing the set of friction surfaces should be as accurate as possible. When a system is represented in terms of truncated modal coordinates, equation (2), a problem could arise if modes describing the motion of the friction surfaces have been truncated. This truncation would effectively constrain the system, yielding an incorrect displacement field and, consequently, an erroneous friction solution. In order to avoid or minimize this inaccuracy, a correction known as residual flexibility (ref. 2) may be applied to the friction DOF. This is basically an attempt to approximate the contribution of truncated higher order modes to the system response. The application of this procedure necessitates modifications to equation (2) as follows:

$$\begin{bmatrix} K_Q + \phi_b^T G_{\rho bb}^{-1} \phi_b & -\phi_b^T G_{\rho bb}^{-1} \\ -G_{\rho bb}^{-1} \phi_b & G_{\rho bb}^{-1} \end{bmatrix} \begin{Bmatrix} q \\ \bar{u}_b \end{Bmatrix} + \begin{bmatrix} M_Q & 0 \\ 0 & 0 \end{bmatrix} \begin{Bmatrix} \ddot{q} \\ \ddot{\bar{u}}_b \end{Bmatrix} = [\Phi_\rho]^T \begin{Bmatrix} F \\ 0 \end{Bmatrix} \tag{17}$$

where

$$\Phi_\rho = \begin{bmatrix} \phi_i - \bar{G}_{\rho ib} G_{\rho bb}^{-1} \phi_b & \bar{G}_{\rho ib} G_{\rho bb}^{-1} \\ 0 & I \end{bmatrix} \tag{18}$$

is the corrected system transformation matrix. The terms $G_{\rho bb}$ and $\bar{G}_{\rho ib}$ are as defined as follows

$$\bar{G}_\rho = \begin{bmatrix} G_{\rho ii} & G_{\rho ib} \\ G_{\rho bi} & G_{\rho bb} \end{bmatrix} \tag{19a}$$

$$\bar{G}_{\rho ib} = \begin{bmatrix} G_{\rho ib} \\ G_{\rho bb} \end{bmatrix} \tag{19b}$$

where $\bar{G}\rho$ is the full residual flexibility matrix. In these equations, the subscript b refers to friction related DOF, while i refers to all other DOF. The matrix K_Q represents the original generalized stiffness matrix (ω^2), while M_Q is the generalized mass matrix (identity). Note that the damping terms have not been included for the sake of brevity. Substitution of equations (17) and (18) into equation (3) yields the nonlinear system equations that are now densely populated.

Applying this integration scheme to these equations is very costly because the required matrix decompositions and multiplications are functions of matrix density. This situation may be remedied by recalling that such a system can be uncoupled through a matrix transformation. The required transformation matrix can be obtained by solving the eigenproblem associated with equation (17) and retaining all modes; however, this approach, is feasible only if the system mass matrix is positive definite. The mass matrix in equation (17) contains null terms at friction surface DOF and is thus nonpositive definite. This problem can be avoided by applying a residual mass correction to the friction surface DOF. The residual mass correction, which is entirely analogous to the residual flexibility correction, results in the equation

$$\begin{bmatrix} K_Q + \phi_b^T G_{\rho bb}^{-1} \phi_b & -\phi_b^T G_{\rho bb}^{-1} \\ -G_{\rho bb}^{-1} \phi_b & G_{\rho bb}^{-1} \end{bmatrix} \begin{Bmatrix} q \\ \bar{u}_b \end{Bmatrix} + \begin{bmatrix} M_Q + \phi_b^T M_{\rho bb} \phi_b & -\phi_b^T M_{\rho bb} \\ -M_{\rho bb} \phi_b & M_{\rho bb} \end{bmatrix} \begin{Bmatrix} \ddot{q} \\ \ddot{\bar{u}}_b \end{Bmatrix} = [\Phi_\rho]^T \begin{Bmatrix} F \\ 0 \end{Bmatrix} \tag{20}$$

in which $M_{\rho bb}$ is the partition of the residual mass matrix related to friction DOF. The eigensolution of equation (17) should yield a set of modes consisting of the original modes appended by a set of residual modes corresponding to the friction DOF. The generalized mass and stiffness matrices associated with this new set of modes is completely diagonal and may be used, with the appropriate transformation matrices, in equation (2). The final result is a system of nonlinear equations that is relatively sparse.

If the residual mass matrix is unavailable, the mass matrix in equation (14) can still be made positive definite by substituting a diagonal matrix containing terms of relatively small magnitude (S) for M. Equation (17) can then be rewritten as

$$\begin{bmatrix} K_Q + \phi_b^T G_{\rho bb}^{-1} \phi_b & -\phi_b G_{\rho bb}^{-1} \\ -G_{\rho bb}^{-1}\phi_b & G_{\rho bb}^{-1} \end{bmatrix} \begin{Bmatrix} q \\ \bar{u}_b \end{Bmatrix} \begin{bmatrix} M_Q & 0 \\ 0 & S \end{bmatrix} \begin{Bmatrix} \ddot{q} \\ \ddot{u}_b \end{Bmatrix} = [\Phi_\rho]^T \begin{Bmatrix} F \\ 0 \end{Bmatrix} \tag{21}$$

The eigensolution of equation (21) should yield results that are almost identical to those obtained using residual mass if S is properly chosen.

Once the corrected equations of motion have been generated, they may be used in equations (15) and (16) such that q is a subset of $\bar{u}_F$. $\bar{u}_b$ in equation (20) includes the friction DOF $\bar{u}_I$ and $\bar{u}_D$. The resulting system equations now provide a much more accurate representation of the friction surfaces. Since there are 2^N possible friction states, there must be 2^N corresponding sets of modal data. These are defined by the constraint equations as a function of the transient solution. In this way, variations in modal content may be effected by merely changing the constraint equations.

TRANSIENT RESPONSE DYNAMICS MODULE MODIFICATIONS

The capability to solve the nonlinear equations of motion with friction forces in NASTRAN required extensive modification to the TRD module. A general approach and an overview of the logic that was adapted is illustrated in figure 2. The logic path on the left of this figure represents the original TRD module with one additional test for a friction solution approach. The logic path to the right represents the requirements when friction forces are evaluated. The nonlinear force output data appears in both logic paths with one significant variation. Output for the nonlinear forces with friction effects occurs after the integration step because the static friction force is a term included with the displacement data.

Two essential ingredients are necessary to evaluate the nonlinear solution when friction is introduced. It is first necessary to monitor the friction forces (f_s and f_k). Secondly, it is required to adjust the coefficients of the constraint equations during the transient solution. For any friction state, the finite difference equation with all nonlinear dependent terms is of the form expressed in equation (12). Because of friction solution requirements, the stiffness operator coefficients, which is $\bar{\bar{K}}$ in equation (12), will change whenever the friction state changes.

In typical orbiter payload transient loads analyses, $\bar{\bar{K}}$ will be of order 400 to 800 and any number of friction state changes will occur. A friction state change requires a change in the coefficient matrix, $\bar{\bar{K}}$; therefore, a solution of equation (12) would require the inverse of $\bar{\bar{K}}$ whenever the friction state changes. A solution approach without further study was defined as not feasible because of economic considerations for matrix coefficients of order 400 to 800.

Computational expense is reduced significantly by noting the following: the changes in $\bar{\bar{K}}$ are local in the matrix array, and equation (12) has the form of a statics problem. Thus, the finite difference formulation lends itself to the method of static condensation (ref. 3). Equation (12) is partitioned as follows:

$$\begin{bmatrix} \bar{\bar{K}}_{ii} & \bar{\bar{K}}_{if} \\ \bar{\bar{K}}_{fi} & \bar{\bar{K}}_{ff} \end{bmatrix} \begin{Bmatrix} \bar{u}_i \\ \bar{u}_f \end{Bmatrix}_{n+1} = \begin{Bmatrix} \bar{\bar{P}}_i \\ \bar{\bar{P}}_f \end{Bmatrix}_{n+1} \tag{22}$$

In equation (22), $\bar{u}_f$ is the DOF set needed to define the friction state and $\bar{u}_i$ is the set of all remaining DOF. Two sets of simultaneous equations are represented by equation (22).

If u_i is eliminated and the time step subscript is dropped for simplicity, the following expressions are obtained.

$$[\bar{\bar{K}}_{ff}] = [\bar{\bar{K}}_{ff}] - [\bar{\bar{K}}_{fi}][\bar{\bar{K}}_{ii}]^{-1}[\bar{\bar{K}}_{if}] \tag{23}$$

$$\{\bar{\bar{P}}_f\} = \{\bar{\bar{P}}_f\} - [K_{fi}][\bar{\bar{K}}_{ii}]^{-1}\{\bar{\bar{P}}_i\} \tag{24}$$

$$[\bar{\bar{K}}_{ff}]\{\bar{u}_f\} = \{\bar{\bar{P}}_f\} \tag{25}$$

The solution for the friction dependent functions, $\bar{u}_f$, is now tractable for any friction state. Essentially, the approach requires an iterative solution of a much smaller set of equations in which the coefficients are adjusted to satisfy

$$\{f_s\} \leq \{f_k\} \tag{26}$$

Equation (26) is a set of constraint variables for an acceptable solution to equation (25). The minimum friction force is selected as the optimum at each friction surface for all trial solutions. Solutions of linear equations with constraint variables similar to those represented by equations (25) and (26) are discussed in ref. 4.

Since an iterative solution procedure is used on a set of variables to obtain particular solutions for equation (25), a criteria is required for changing friction states. All friction force variables that have a relative velocity near zero are first assumed to be in a static friction state. The coefficients of equation (26) as well as the appropriate $\overline{P_f}$ term are adjusted accordingly. A trial solution is obtained. When multiple friction surfaces do not satisfy equation (26), the friction surface reflecting a static friction force, f_s, which is greater than the kinetic friction force, f_k, by the largest percentage is changed to a sliding state and the kinetic friction force is used in the solution of equation (25). Because the relative velocity is by definition zero during stiction dwells, the sign of the kinetic friction force is also assumed to have the same sign as the static friction force for transition from a stuck state to a sliding state. Thus, equation (26) is satisfied by obtaining a particular solution derived from a constant relative displacement criteria, as illustrated in equations (15) and (25). If equation (26) cannot be satisfied, the solution form represented by equation (16) is chosen and the kinetic friction state is assumed. The solution for the $\bar{u}_i$ set is obtained from the following:

$$\{\bar{u}_i\} = [\bar{K}_{ii}]^{-1}\{\bar{P}_i\} - [\bar{K}_{ii}]^{-1}[\bar{K}_{if}]\{\bar{u}_f\} \tag{27}$$

Table I defines all subroutine functional characteristics in relation to each modified or new subroutine implemented for solving the transient response with static and kinetic friction forces. It begins wtih the DMAP module, TRDNL, which is an expanded version of the original TRD module. All subroutines and subroutine entry points to perform discrete functions are identified in a logical path from initialization through the computational sequence and on to the specific friction solution iterative subroutine, DUDEQZ. In addition, all subroutines are identified as either modified NASTRAN fortran code or newly developed fortran code. Data are also provided that indicate the degree of difficulty incurred in developing or implementing the specific subroutine even though this may have a personal bias.

An additional feature that was implemented required special and unique provisions in subroutine TRD1D. Specific scaler values on NOLIN bulk data were used for two special purposes not defined by NASTRAN. The use of specific scaler values also allows all necessary input data modifications to remain local to the TRD module as opposed to also modifying the input processing region of NASTRAN and passing specific data to the TRD module. The first special purpose scaler value was defined to generate a vector sum of two variables, such as the root-sum-square of two forces. This provided the capability to evaluate a normal force as a function of two independent variables, which is required to define the kinetic friction force in equation (14). A second function embedded in subroutine TRD1D defines sets of variables for each of the friction surfaces. By combining the definitions of each of the friction surface sets, it is possible to define a system partition vector. These data provide the appropriate definitions for initialization of the finite difference coefficient matrices as well as partitioning data, coefficient matrix manipulations, and solution procedures to solve the system of equations in a partitioned form, which is indicated by equation (22). The partitioning data are also used to monitor the friction solution states in subroutine DUDEQZ.

Thus, NASTRAN's capability is expanded to modify the finite difference form of the equations of motion by using constraint equations. The constraints are further modified by a solution logic choice between static friction or kinetic friction during the finite difference integration process. In addition, static condensation of the finite difference coefficient matrix is implemented to reduce the computational cost of solving for the friction state and the resultant friction forces.

FRICTION DEMONSTRATION PROBLEM

The primary intent of this demonstration problem is to illustrate the effects of modal truncation on dynamic response data when friction forces are included. A secondary intent is to examine friction methodologies that can be effectively implemented for payload loads analyses.

For simplicity, a one-dimensional problem was developed consisting of masses connected by springs, as shown in figure 3. Also included in figure 3 are the physical properties required to generate the structural model. Basically, it consists of 23 DOF interconnected by linear springs and includes three friction surfaces.

Four approaches to solve this transient response problem with friction were studied. The four solution approaches, which are also summarized in table II are:

1. Solve the problem in the physical coordinate system.

2. Solve the problem using a truncated mode set; (two sets of results are presented later): one set using 12 of the possible 23 modes and another set using 18 of the possible 23 modes.

3. Solve the problem using the same truncated modes as solution approach 2 (12 mode set), but include residual flexibility corrections for the friction surfaces.

4. Solve the problem using the same truncated modes as solution approach 2 (12 mode set), but include both residual mass and flexibility corrections for the friction surfaces.

These transient response solutions will be referred to as solution approaches 1 through 4 in the following discussions. Solution approach 1 is considered as a reference solution to which solution approaches 2 through 4 are compared to understand the effects of modal truncation on the transient response solution when friction forces are also included. The methodology used in solution approaches 3 and 4 is identical to that which Rockwell has employed for payload loads analyses.

Figures 4 through 8 are selected response terms for the four different approaches to solving the transient response problem and figure 9 is the time history plot of the applied forcing function at block 7 in figure 3. It is appropriate to note that all response data not shown demonstrates results similar to those depicted by these selected response terms. Also, the first approach (i.e., no modal truncation) was solved using all 23 system modes and the transient response solution was essentially identical to that obtained using physical coordinates. The natural frequencies for this friction demonstration problem are included in table III.

There is a serious degradation when solution approach 2 (i.e., a modal transformation that approximates the system with 12 and 18 of the possible 23 modes of vibration) is compared to any of the other three solution approaches. It is a preferred method for linear transient response solutions and is particularly useful for large finite element models, but figures 4 through 8 indicate distortions in the response data. The friction force time histories, which are shown in figure 6, indicate a potential degradation to the stiffness characteristics of the system because of a more rapid change of the friction force when the modally truncated solution is compared to the solution that uses physical coordinates. These observations tend to indicate a difficulty with the friction surfaces alone. They also suggest that something was deleted from the system synthesis by solely transforming to generalized coordinates, as was done in solution approach 2.

Residual flexibility data for the friction DOF provides a measure of the flexibility loss when a truncated modal transformation is used. Conversely, it indicates the degree of stiffening brought about by the truncated modal transformation. For this demonstration problem, these data are presented in table IV and provide a qualitative measure of the flexibility loss at the friction surfaces when the 12 modes that were used in solution approach 2 are compared to the total flexibility of the structural system (i.e., 23 modes). Except for block 27, the flexibility loss data suggests a severe truncation approximation has taken place for all friction surfaces. The flexibility data also suggest that difficulties may be encountered in arriving at a realistic solution when a compatibility assessment for the friction surfaces during a transient response solution is required.

When physical displacement data are approximated by truncated system modes times the generalized displacements, the relative displacement terms used to evaluate the friction force data are likely to be distorted. Since relative displacements for the friction surfaces are equal to the difference of two physical displacement terms, the transient response data are likely to be distorted when the two physical displacements are approximated to different levels of accuracy. This situation is indicated by a comparison of the truncated flexibility percentage data for blocks 17 and 27 in table IV. The approximation to different levels of accuracy may be a contributing factor to the relative displacement

distortions for the friction surfaces, such as indicated in Figure 4, when there are extended dwells at a constant relative displacement.

Therefore, it is hypothesized that the friction forces, when derived as a function of relative displacement terms that are obtained from a structural system that is too stiff, will be distorted when compared to a factual solution, such as solution approach 1. Illogical consequences in a transient response analysis with friction could be significant, as evidenced by the results using truncated modes only and the related time history response data comparisons. Thus, when related to a friction surface, the relative displacements should not retain a significant local stiffness approximation for transient response solutions with friction forces included if a significant flexibility loss is noted for the friction DOF. As presented in table III, the flexibility loss ratio data are variables required to recognize when such a situation exists.

The previous discussions suggest that the modal transformation approximation implemented in solution approach 2 be enhanced before the transient solution with friction is attempted. Because a compatibility assessment is required to evaluate the stiction friction force during periods of zero or near-zero relative velocity, it is also suggested that the transient response will likely be distorted unless the friction DOF are corrected to reflect valid local system stiffnesses. Solution approaches 3 and 4 are formulated to alleviate the difficulty of acquiring a quality compatibility assessment for the friction surfaces. The modal transformation from physical to generalized coordinates is accomplished first. Afterwards, an enhancement to the relative displacements for the friction surfaces is performed by a residual flexibility correction for solution approach 3 (see equation (21)), and by both a residual flexibility and mass correction for solution approach 4 (see equation (20)).

Evidence that the system stiffness characteristics are enhanced by implementing solution approaches 3 and 4 may be observed by inspecting any of the time history plots. Of particular significance are the variations in the friction force time histories (see figure 6). It is noted that these time history data for solution approaches 3 and 4 are nearly identical to the more exact representation when physical coordinates are employed (solution approach 1). Since the variation in the relative displacements and the friction forces has virtually vanished, the conclusion is that a valid compatibility description is now maintained at the friction DOF.

It is appropriate to specifically note the response characteristics of accelerations and element force time history data because they provide an indication of the solution impact on payload acceleration transformation matrix (ATM) and load transformation matrix (LTM) response recovery data. The acceleration item recoveries for mass item 35, shown in figure 7, has significant amplitude deviations as well as slight phase shifts when solution approach 2 is compared to solution approaches 1, 3, and 4. Solution approaches 3 and 4 may have amplitude deviations when compared to the reference solution, but they are difficult to measure by eye. Any apparent amplitude distortions of solution approaches 3 and 4 would appear to be minor when the larger approximation introduced by the truncated modal solution, solution approach 2, is compared to the reference solution. The selected element force time histories exhibit similar distortions, as indicated in figure 8 for solution approach 2, and are improved in solution approaches 3 and 4 when compared to solution approach 1. These data comparisons indicate that ATM and LTM response recovery data for payloads could be altered if one did not adjust the modally truncated system stiffness characteristics to acquire a valid compatibility assessment at the friction surfaces. It is not implied that the percentage differences would be identical or even close to what is indicated by these data but rather that a truncated modal transformation would alter the transient response solution by employing a degenerative compatibility description for the friction surfaces.

From the results of this demonstration problem, it is observed that solution approach 2, which relies only on a set of modally truncated generalized coordinates, significantly distorts the dynamic behavior of the transient response solution with friction forces. Evidence that a system flexibility degradation is present is deduced by inspecting the residual flexibility data for the friction DOF. Both the residual flexibility and the residual mass adjustments tend to alleviate the response distortions by enhancing the structural system stiffness characteristics so that a quality compatibility assessment for the friction surfaces can be maintained during the transient solution. All time history plots indicate that both solution approaches 3 and 4 tend to converge to the results obtained from solution approach 1, the reference solution.

APPLICATION TO LARGE FINITE ELEMENT PROBLEMS

The methodology presented here has been implemented in several Space Shuttle payload transient loads analyses. These problems are generally large, typically on the order of 1,200 physical DOF. In order to reduce solution costs to a more reasonable level, the transient loads analysis is usually solved in truncated modal coordinates. The cutoff frequency

may range from 35 to 50 Hertz. While this representation may be adequate for a linear analysis, a severe loss in flexibility at the orbiter payload friction interfaces is generally experienced. Table V illustrates the loss in flexibility that occurred in a typical Space Shuttle/IUS coupled modal model. Therefore, residual flexibility corrections are necessary in order to ensure a valid solution, as illustrated in the demonstration problem. Results for an analysis conducted with and without residual flexibility corrections are also presented in figures 10 and 11. The stiffening effect of truncation on the friction interface results in a more rapid static friction force response to a dynamic loading. Figure 10 illustrates this effect. Figure 11 depicts the total friction force (static plus kinetic) time history corresponding to figure 10. A comparison of the data suggests that the dynamic input from the friction forces into the system can be radically altered by modal truncation.

The costs associated with a friction analysis are significant in a large-order problem because of the requirements for a small integration step size and the number of matrix operations involved; however, data from several loads analyses indicate that friction may have a major impact on payload component responses. Tables VI and VII present results for two spacecraft cantilevered from the IUS. The data consists of the maximum accelerations experienced by spacecraft components for an analysis conducted with and without the effects of friction. Table VI contains data for the tracking and data relay satellite (TDRS) 11 spacecraft for a lift-off transient event while table VII contains similar data for the DSCS-III/DSCS-III spacecraft based on overall landing transient maximums. The primary difficulty with these data is to recognize that the percentage variations are as large if not larger than uncertainty factors that are generally employed in linear loads analyses, which presents the payload designer with a dilemma. Thus, it appears as though it may be justified to investigate friction effects in a transient loads analysis.

FRICTION SOLUTION

The friction solution is outlined as follows.

1. The equations of motion are prescribed as outlined in equation (4). Static constraint equations are applied as illustrated in equation (15) with static friction on all trunnions as the initial friction state.

2. The friction DOF in equation (4) are augmented by use of residual flexibilities to correct for modal truncation errors (equation(21)). The initial displacements are calculated such that f_s is zero.

3. Either residual mass or a small fictitious mass is applied to the mass matrix, an eigen analysis is performed, and the equations of motion are transformed to this new modal coordinate system with no truncation. Any numeric round-off error in the rigid body modes is eliminated.

4. The transient solution is executed and the constraint equations are adjusted according to programmed solution logic that chooses between stiction and sliding friction states as required (equations (15) and (16)). The method of static condensation (equations (22) through (25)) is employed to minimize computational cost of the required matrix inversion whenever the friction state changes.

CONCLUSIONS

The methodology presented allows an analyst to include aspects of the friction phenomenon neglected in some other approaches. In particular, use of the total flexibility on the friction DOF is a necessity if the static friction forces and the corresponding payload response are to be accurately represented. Implementation of residual flexibilities with the appropriate constraint equations lead to an accurate representation of the modal content for each particular friction state and appears to be a logical extension of a linear loads analysis that has used truncated modal coordinates. Static condensation on the recurrence equation provides efficient and cost effective adjustment of the equations of motion any time the friction state changes. Also, diagonalizing the equations of motion and retaining the complete set of modes (i.e., original plus residual) leads to a substantial cost savings with no apparent degradation of the analytic results.

The method is generally applicable to a large class of transient response problems. It has direct application to problems involving surface contact and separation. In particular, a similar problem of launch vehicle to launch pad separation might also be investigated with this approach if friction forces are considered to be a dominating influence.

Finally, application of residual modes to other transient friction methodologies that have employed truncated modal transforms appears to be feasible. Incorporating residual flexibilities expands the retained modal data by the number of friction DOF. The modified system equations of motion include the total flexibility at the friction interfaces and can be diagonalized a second time. Implementing a residual modes correction will enhance the accuracy of other approaches that presently employ standard truncated modal transforms.

REFERENCES

1. *The NASTRAN Theoretical Manual (Level 17.5).* NASA SP-221(03), general release (Mar. 1, 1979).

2. Rubin, S. "Improved Component-Mode Representation for Structural Dynamic Analysis," AIAA Journal; Vol 13, Number 8 (Aug. 1975) pp. 995-1006.

3. Bathe, Klaus-Jurgen and Sheryl Gracewski. "On Nonlinear Dynamic Analysis Using Substructuring and Mode Superposition," Computers and Structures, Vol 13 (1981) pp. 699-707.

4. Wagner, H. M. *Principles of Operations Research.* Prentice-Hall, Inc.; Englewood Cliffs, N.J. (1975).

5. Henkel, E. E., J. E. Misel, and D. H. Frederick. "A Methodology to Include Static and Kinetic Friction Effects in Space Shuttle Payload Transient Loads Analysis." Presented at AIAA Shuttle Environment and Operations Meeting, Washington, D.C., (Oct. 3, 1983).

TABLE I. — FUNCTIONS ASSIGNED TO SUBROUTINES FOR THE TRD MODULE WITH FRICTION FORCES

NASTRAN subroutine			Degree of difficulty*	Subroutine function/comment
Name	Modified	New		
TRDNL	X		1	Modified TRD module with additional entry parameters, scratch files, and control logic for new subroutine processing and additional initialization for static condensation.
TRD1C	X		3	Modified NASTRAN computational control subroutine to implement the finite difference algorithm. When friction forces are defined the following capabilities are activated: • Evaluate the finite difference recursion formula by static condensation • Evaluate the friction state and forces • Output nonlinear forces corrected for friction state
TRD1CI	X		1	This is a new entry in subroutine TRD1C, which calls subroutine TRD1D to inspect the NOLIN bulk data inputs for friction definitions. If friction inputs are defined, a partition vector is output to a scratch file.
TRD1CN		X	2	This new entry in subroutine TRD1C, which forms the appropriate coefficient matrices for the friction problem, inspects the partition vector, and prepares to solve the finite difference algorithm by parts.
GENPVF		X	1	This subroutine writes a NASTRAN-type partition vector to a specified scratch file.
INITIL	X		2	This subroutine forms the finite difference equation coefficient matrices (equation (11)). If friction is defined, it prepares to partition, $\bar{K}$, in equation (12).
INITLD	X		2	Entry point in subroutine INITL to decompose K_{ij} of equation (22) if friction is defined. It also completes the finite difference coefficient matrix computation when a friction solution is specified.
PARTKC		X	2	Partition the finite difference coefficient matrix, $\bar{K}$, in equation (12) for a static condensation solution, as indicated in equation (22).
FINITL		X	2	This subroutine is required to finish initialization when a friction solution is required and a static condensation solution procedure is in process. It prepares matrix products for solution of equations (23), (24), and (27).
CFBSOR	X		1	NASTRAN forward-backward substitution subroutine for solution of linear equations.
CFBSOF	X		1	Entry in subroutine CFBSOR to alter memory allocation.

TABLE I. — FUNCTIONS ASSIGNED TO SUBROUTINES FOR THE TRD MODULE WITH FRICTION FORCES (CONT)

NASTRAN subroutine			Degree of difficulty*	Subroutine function/comment
Name	Modified	New		
TRD1D	X		3	This subroutine performs the following functions: • Allocate memory for nonlinear functions • Initialize tabular data tables • Evaluate friction definitions, if any • Evaluate nonlinear functions • Calculate nonlinear force data It was modified extensively to recognize specific scaler values of the NOLIN1 and NOLIN2 bulk data types, alter memory allocation, process a root-sum-square force term of the type required for kinetic friction forces, and monitor friction solution states in regions of near-zero relative velocity.
TRD1DF	X		3	This is a new entry in subroutine TRD1D to update the nonlinear force data when a friction state change is indicated by subroutine DUDEQZ.
STEP	X		3	Subroutine STEP controls the numerical evaluation of the finite difference recursion relation shown in equation (11). It was expanded to support static condensation evaluation requirements.
STEP2A		X	3	Entry in subroutine STEP to evaluate the inverse matrix product in equation (24).
STEP2B		X	3	Entry in subroutine STEP to complete the evaluation of equation (24).
STEP2C		X	3	Entry in subroutine STEP to evaluate the displacement data of equation (27)
MATVEC	X		1	Subroutine MATVEC forms the product $X = X + Ay$, where A is a matrix and y is a vector.
NEVGEC		X	2	Entry in subroutine MATVEC to form the product $X = X - Ay$, where A is a matrix and y is a vector.
DUDEQZ		X	3	This subroutine is the iterative solution control subroutine to evaluate equation (25) with the friction solution constraints presented in equation (26).
NLCMXR		X	2	A subroutine to adjust the constraint relationships for static and kinetic friction force solution requirements. The row terms for a constraint relationship (see equation (15)) are set to zero and the appropriate diagonal is set to unity (see equation (16)).

TABLE I — FUNCTIONS ASSIGNED TO SUBROUTINES FOR THE TRD MODULE WITH FRICTION FORCES (CONT)

NASTRAN subroutine			Degree of difficulty*	Subroutine function/comment
Name	Modified	New		
FI2FPN	X		2	This subroutine locates specific terms for the solution of equations (25) and (26). It provides the capability to locate particular friction surface, quantities such as a static friction force term.
GDEC		X	2	This subroutine prepares to solve a set of linear equations of the form AX = B where A is a coefficient array, B is a specified vector, and X is the desired solution. The coefficient array A is triangularized by Gaussian elimination.
GSOL		X	2	This subroutine evaluates the linear system of equations prepared previously by subroutine GDEC.
INCVP		X	1	A subroutine to partition a vector given a NASTRAN-type partition vector. The data are all memory resident.
INCVM		X	1	A subroutine to merge a vector given a NASTRAN-type partition vector. The data are all memory resident.

*1 = Minor
2 = Moderate
3 = Extensive

TABLE II. — DESCRIPTION OF SOLUTION APPROACHES

Solution approach	Solution approach description
1	• A solution approach that retains the displacements, velocities, and accelerations in a physical coordinate system • A finite difference integration procedure is used to generate the time history response data • No damping is used
2	• A solution that employs a modal transformation approximation for the physical displacements, velocities, and accelerations • Only the first 12 of the possible 23 modal vectors are used to approximate the displacements, velocities, and accelerations • No damping is used • A second solution was obtained using 18 of the possible 23 modal vectors
3	• A solution that employs a modal transformation approximation for the physical displacements, velocities, and accelerations • The same 12 modes as selected for solution approach 2 are employed in this solution; however, friction forces were calculated as a function of relative displacement data measured from additional degrees of freedom that have been corrected by residual flexibility functions • No damping is used
4	• This solution approach was identical to solution approach 3 with the addition of residual mass functions to the degrees of freedom retained for the friction force relative displacement data • No damping is used

TABLE III. — FRICTION DEMONSTRATION PROBLEM; NATURAL FREQUENCIES

Mode	Frequency (Hz)
1	1.67
2	2.52
3	4.93
4	5.74
5	7.89
6	8.08
7	10.04
8	10.99
9	12.30
10	12.33
11	13.48
12	14.24
13	70.14
14	70.14
15	70.15
16	70.15
17	70.15
18	70.15
19	70.15
20	70.15
21	70.15
22	70.16
23	221.81

TABLE IV. — FRICTION DEMONSTRATION PROBLEM; PERCENT TRUNCATED FLEXIBILITY

Description*	Percent of total flexibility truncated	
	Upper block*	Lower block*
Blocks 13X	49	N/A
23X	N/A	49
Blocks 15X	25	N/A
25X	N/A	25
Blocks 17X	17	N/A
27X	N/A	2

Modes above 14.24 Hz truncated
*Refer to table III and figure 3.

TABLE V. — IUS-ORBITER FRICTION DEGREES OF FREEDOM; PERCENT TRUNCATED FLEXIBILITY

Description	Percent of total flexibility truncated	
	Orbiter side	IUS side
Forward ASE Y*	43	3
Aft ASE forward Y*	42	16
Coulomb damper Y*	90	6
Coulomb damper Z*	83	2
Aft ASE aft X*	66	79
Aft ASE aft Y*	53	37
Keel Z	51	31

From DSCS/IUS loads analysis, M60W01 orbiter math model, P3B IUS math model, landing condition, modes above 50 Hz truncated (ref. 5)
*Symmetry from right-hand side to left-hand side

TABLE VI. — TDRS-11 COMPONENT ACCELERATIONS COMPARISON OF LIFT-OFF CASE L0942H

Component description	Orbiter direction	Maximum absolute acceleration (g's)		Percent difference
		Frictionless	Friction	
SGL antenna	X	3.062	2.939	−4
	Y	2.754	2.636	−4
	Z	3.131	3.188	2
SGL feed	X	4.877	4.317	−11
	Y	2.276	2.320	2
	Z	5.459	4.861	−11
C-band antenna	X	3.693	3.238	−12
	Y	1.151	1.273	11
	Z	4.015	3.435	−14
Top C-band antenna	X	4.083	3.537	−13
	Y	4.095	3.979	−3
	Z	12.375	9.721	−21
Propellant tank c.g.	X	3.113	3.060	−2
	Y	0.505	0.466	−8
	Z	0.987	1.056	7
+Y solar panel outer hinge	Z	1.277	1.312	3
	Y	3.677	4.795	30
+X solar array antenna	Z	8.461	13.393	58
	Y	12.134	9.596	−21

TABLE VII. — DSCS PAYLOAD COMPONENT ACCELERATION COMPARISON FOR LANDING CASES

Component description	Orbiter direction	Maximum absolute acceleration (g's)		Percent difference
		Frictionless	Friction	
Aft spacecraft:				
Center-body multibeam antenna	Z	2.05	2.23	9
Center-body multibeam antenna	Y	2.13	2.43	14
Center-body tank	Y	2.15	2.28	6
Center-body tank	Z	0.51	0.89	75
Center-body dish antenna	Y	3.17	5.98	87
Center-body dish antenna	Z	2.05	3.88	89
Solar array	Y	2.02	2.22	10
Solar array	Z	2.36	2.68	14
Solar array	Z	2.38	5.94	150
Forward spacecraft:				
Center-body multibeam antenna	Z	2.51	2.49	−1
Center-body multibeam antenna	Y	0.75	0.62	−17
Center-body tank	Y	0.84	0.72	−14
Center-body tank	Z	2.71	1.04	−62
Center-body dish antenna	Y	3.58	3.87	8
Center-body dish antenna	Z	2.72	2.74	1
Solar array	Y	0.79	0.86	9
Solar array	Z	3.01	3.69	23
Solar array	Z	3.47	4.02	16

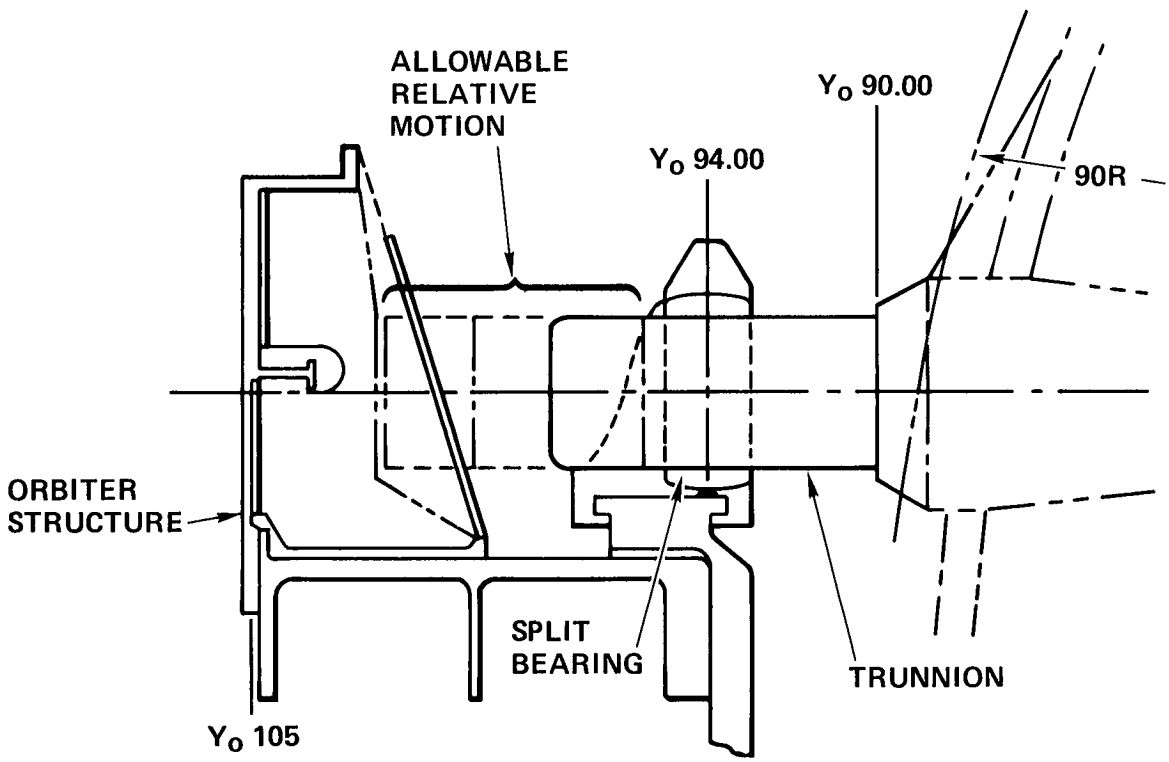

FIGURE 1. — LONGERON ATTACHMENT MECHANISM AND ASSOCIATED PAYLOAD TRUNNION FOR NONDEPLOYABLE PAYLOAD

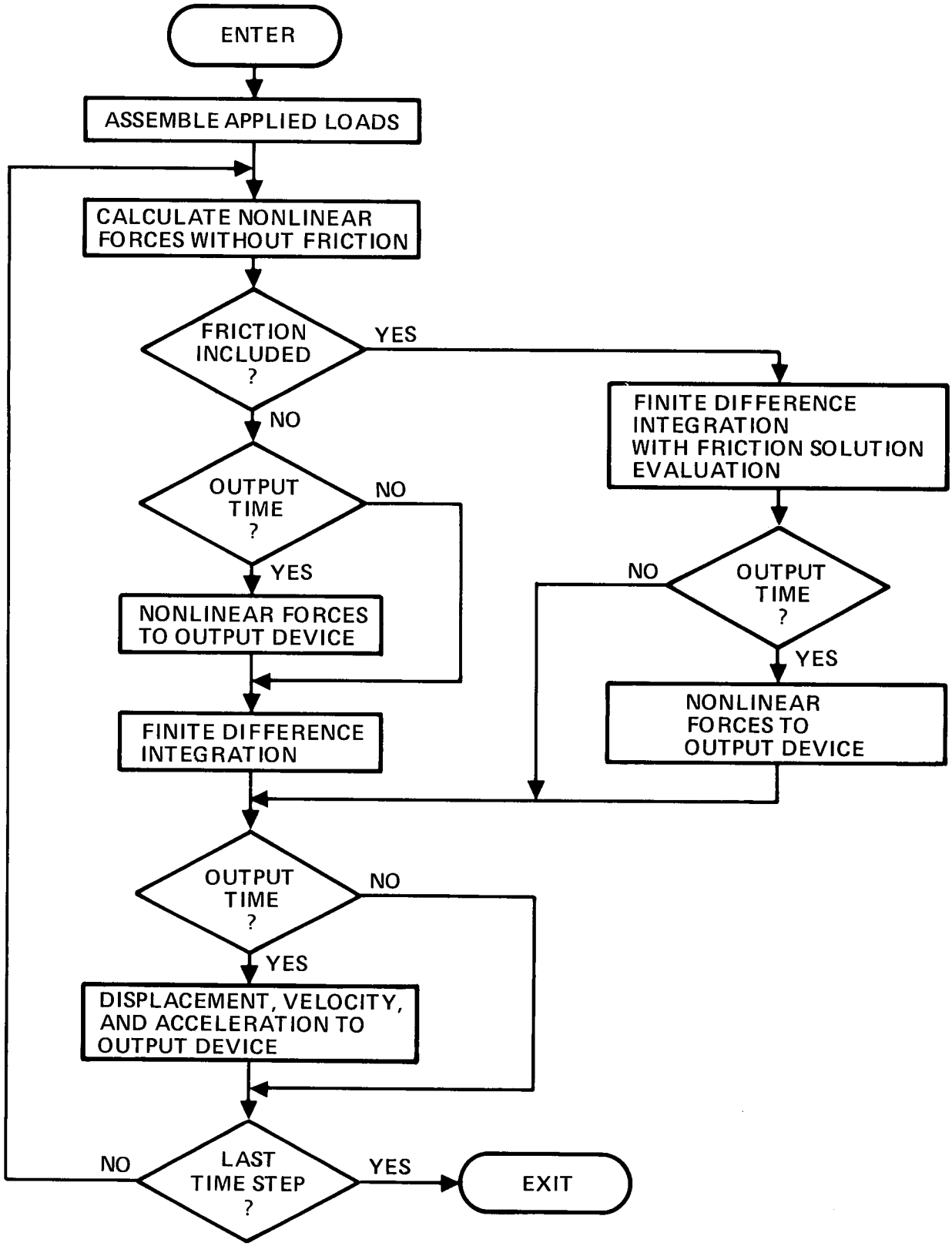

FIGURE 2. — NONLINEAR TRANSIENT RESPONSE WITH FRICTION

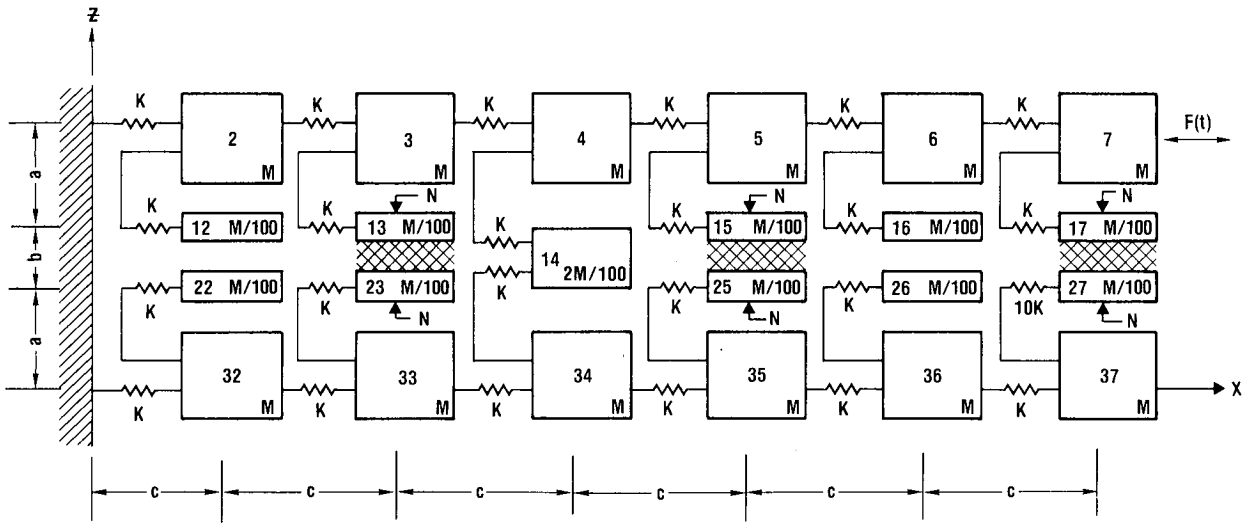

= FRICTION SURFACE
N = NORMAL FORCE = CONSTANT AT ALL FRICTION SURFACES = 10.0 LB
μ = 0.1
M = 0.026 LB-S^2/IN.
K = 50.0 LB/IN.
a = 1.0 IN.
b = 0.5 IN.
c = 10.0 IN.

FIGURE 3. — FRICTION DEMONSTRATION PROBLEM

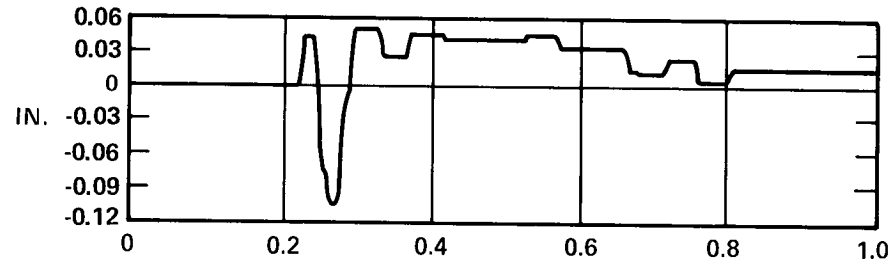

SOLUTION APPROACH 1 (REFERENCE SOLUTION)

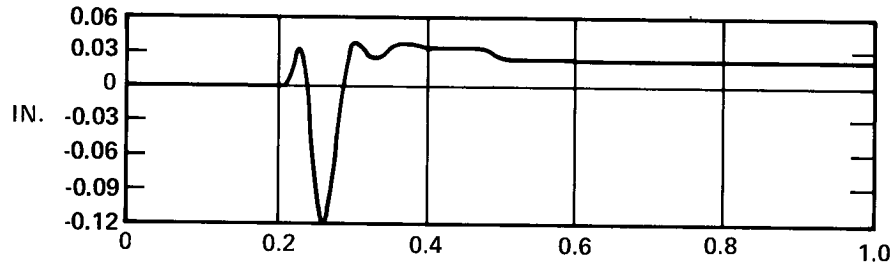

SOLUTION APPROACH 2 (12 MODES)

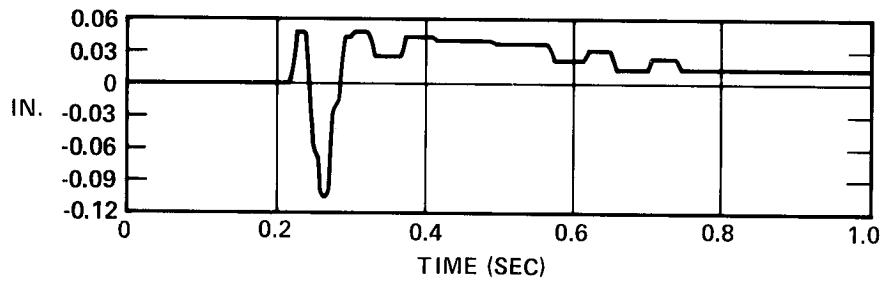

SOLUTION APPROACH 2 (18 MODES)

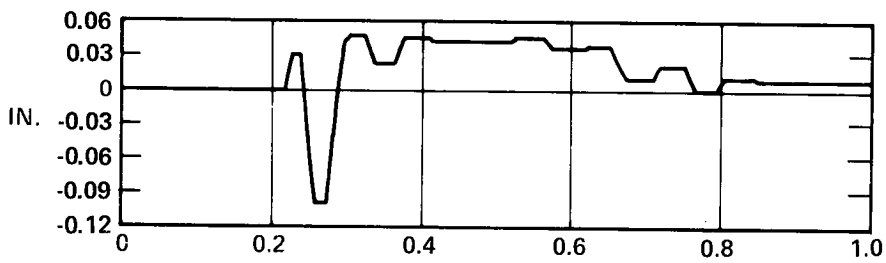

SOLUTION APPROACH 3 (12 MODES WITH RESIDUAL FLEXIBILITY)

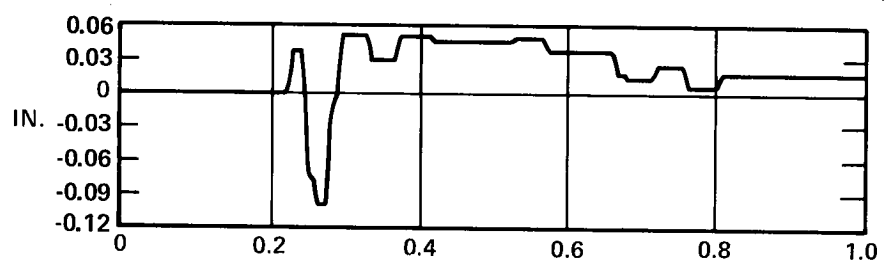

SOLUTION APPROACH 4 (12 MODES WITH RESIDUAL FLEXIBILITY AND RESIDUAL MASS)

FIGURE 4. — RELATIVE DISPLACEMENT; 17/27

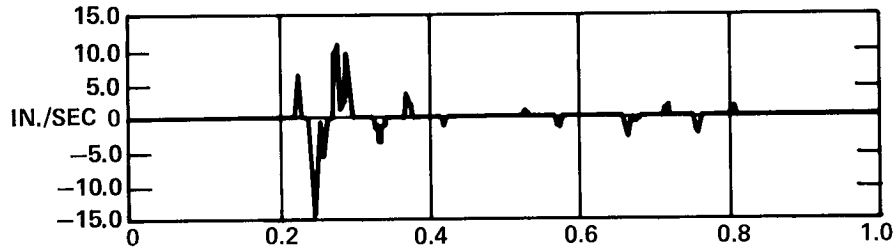

SOLUTION APPROACH 1 (REFERENCE SOLUTION)

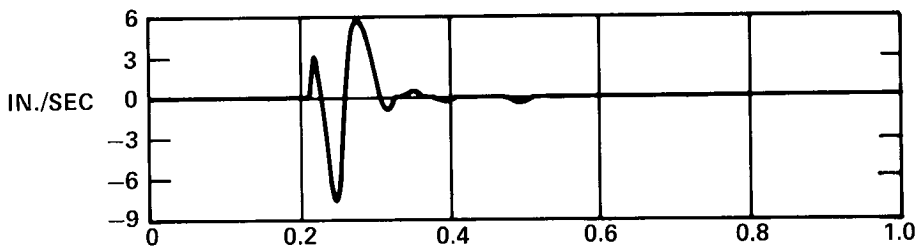

SOLUTION APPROACH 2 (12 MODES)

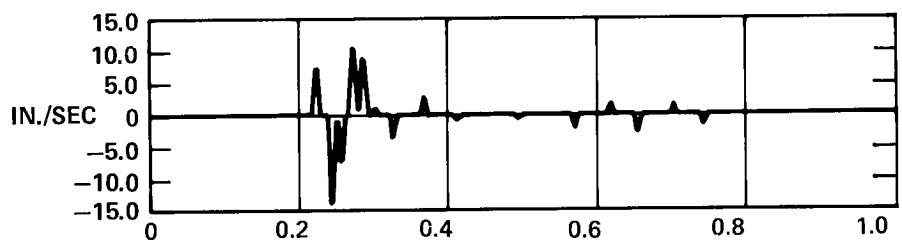

SOLUTION APPROACH 2 (18 MODES)

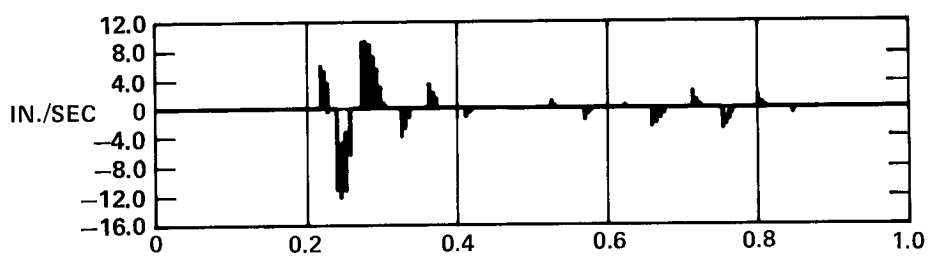

SOLUTION APPROACH 3 (12 MODES WITH RESIDUAL FLEXIBILITY)

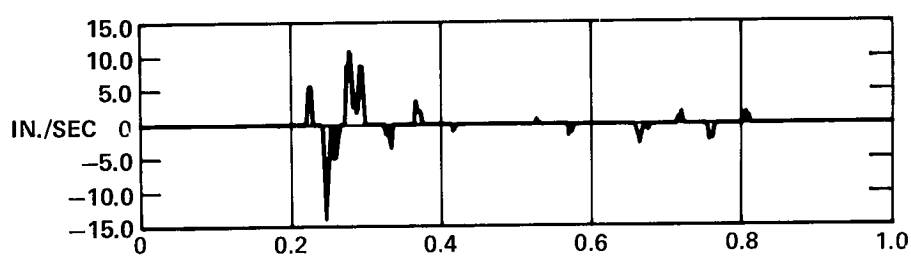

SOLUTION APPROACH 4 (12 MODES WITH RESIDUAL FLEXIBILITY AND RESIDUAL MASS)

FIGURE 5. — RELATIVE VELOCITY; 17/27

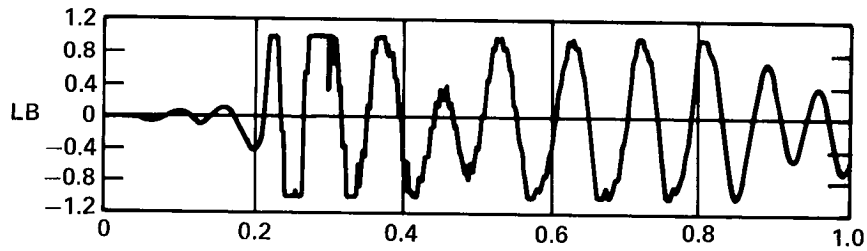

SOLUTION APPPROACH 1 (REFERENCE ONLY)

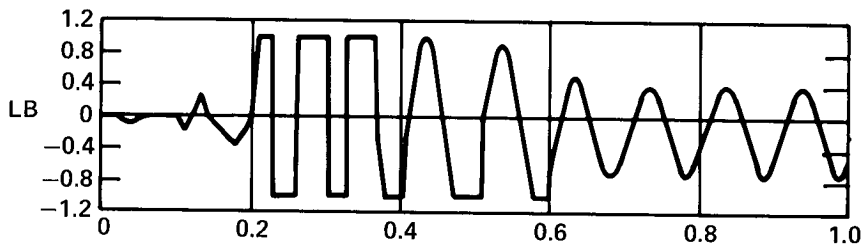

SOLUTION APPROACH 2 (12 MODES)

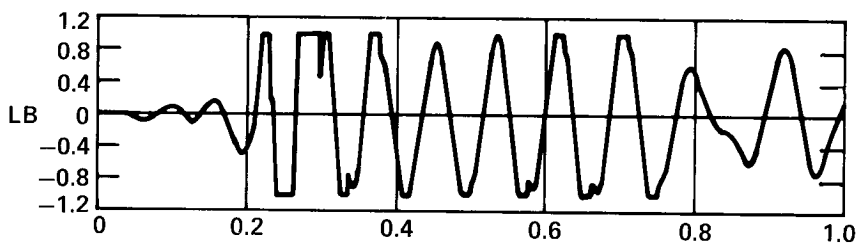

SOLUTION APPROACH 2 (18 MODES)

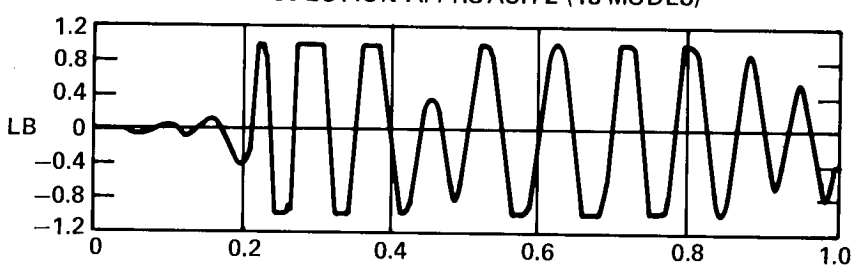

SOLUTION APPROACH 3 (12 MODES WITH RESIDUAL FLEXIBILITY)

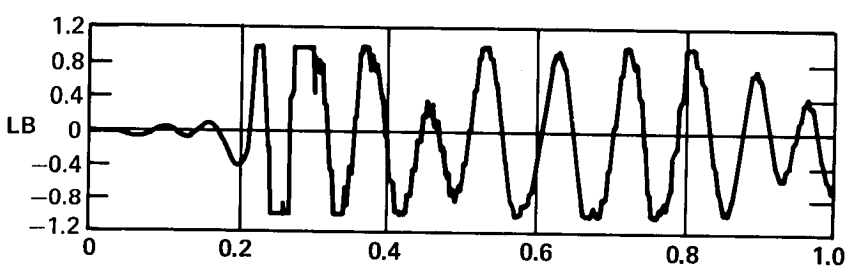

SOLUTION APPROACH 4 (12 MODES WITH RESIDUAL FLEXIBILITY AND RESIDUAL MASS)

FIGURE 6. — FRICTION FORCE; 17/27

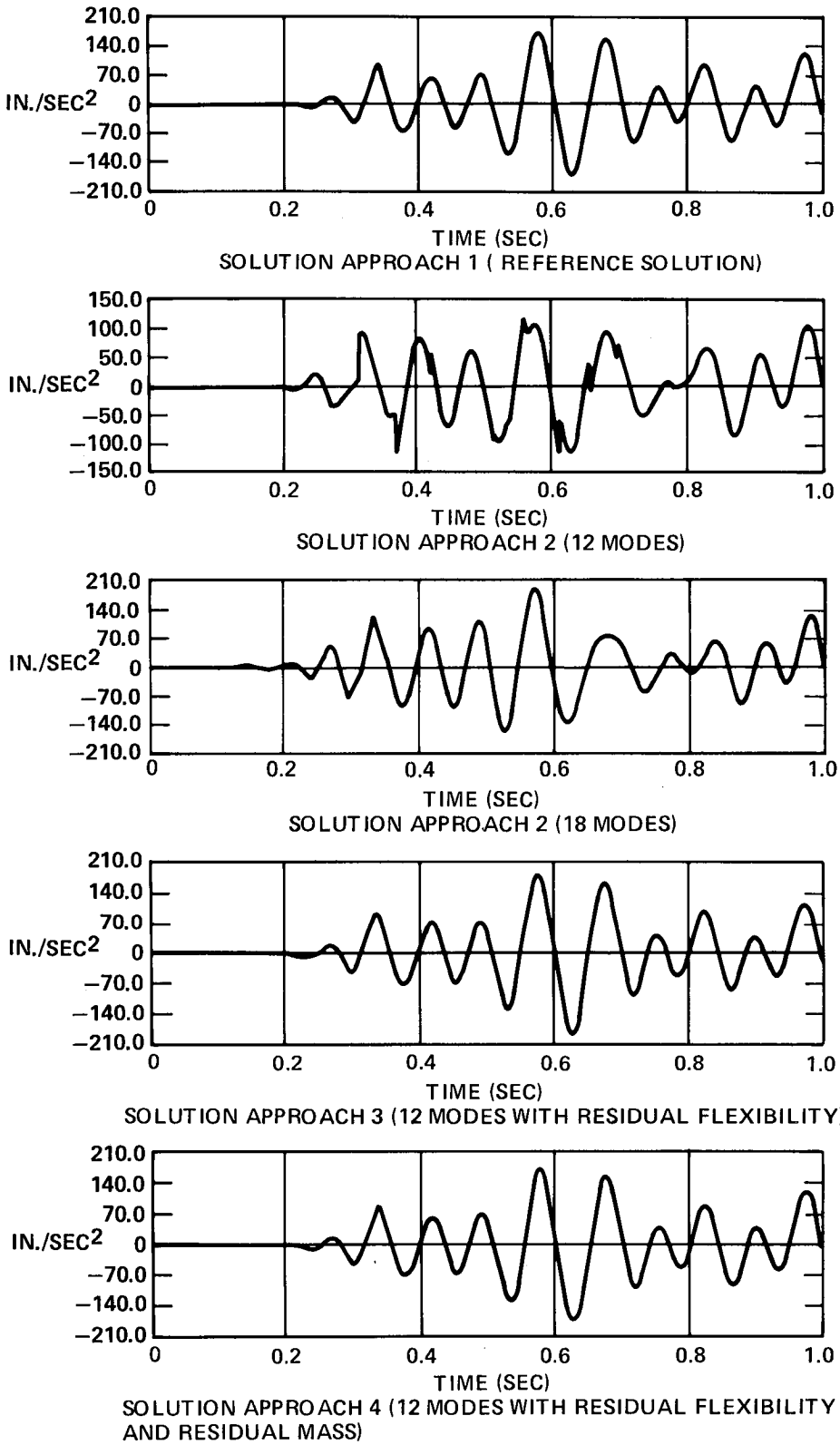

FIGURE 7. — ACCELERATION; 35

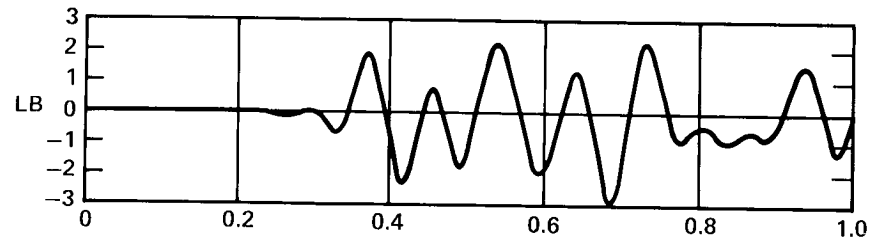

SOLUTION APPROACH 1 (REFERENCE SOLUTION)

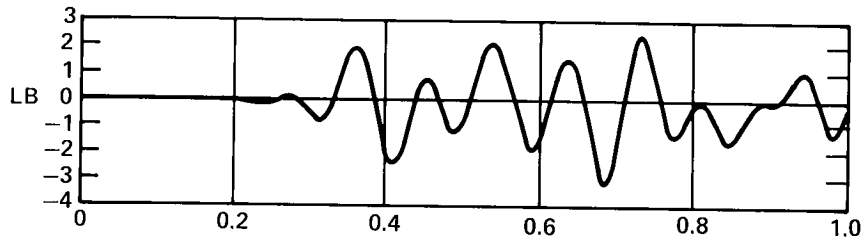

SOLUTION APPROACH 2 (12 MODES)

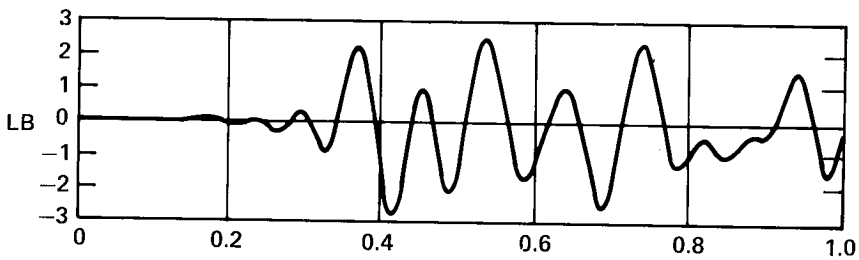

SOLUTION APPROACH 2 (18 MODES)

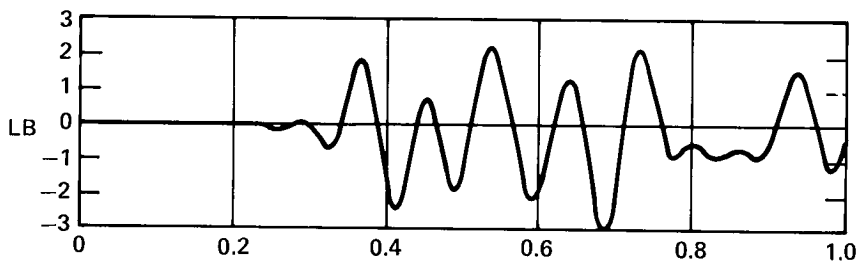

SOLUTION APPROACH 3 (12 MODES WITH RESIDUAL FLEXIBILITY)

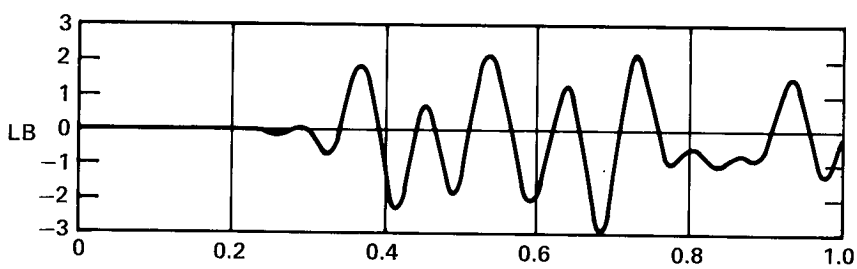

SOLUTION APPROACH 4 (12 MODES WITH RESIDUAL FLEXIBILITY AND RESIDUAL MASS)

FIGURE 8. — ELEMENT FORCE; 34/35

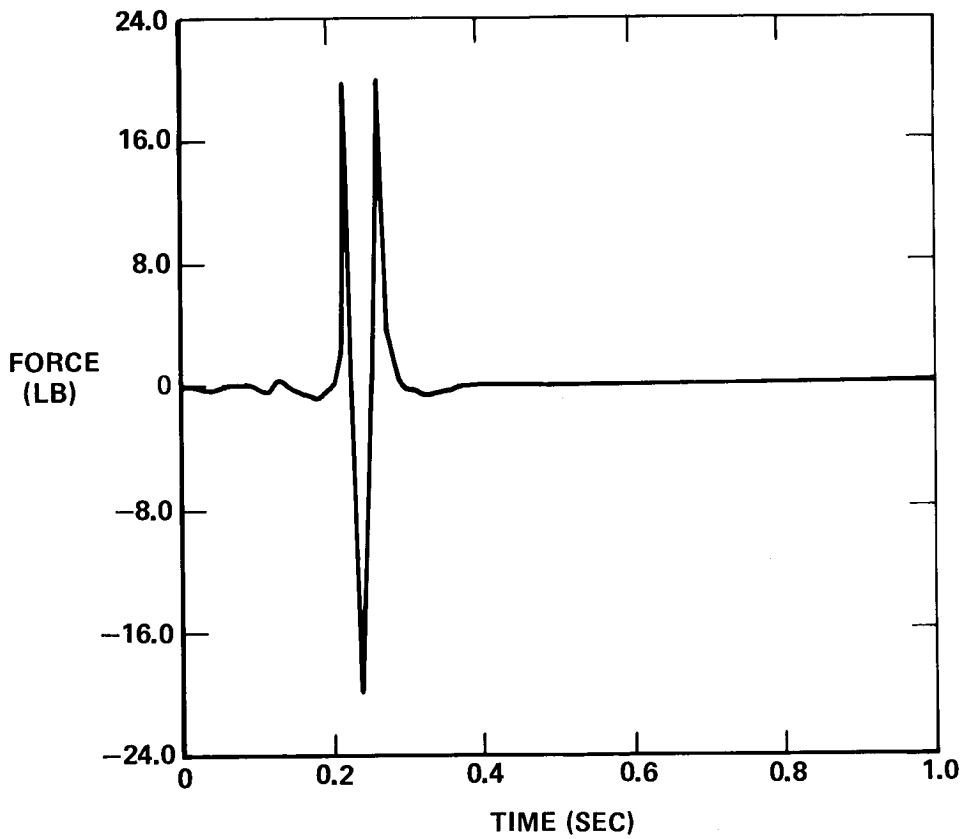

FIGURE 9. — FRICTION DEMONSTRATION PROBLEM WITH APPLIED FORCE; 7 DOF

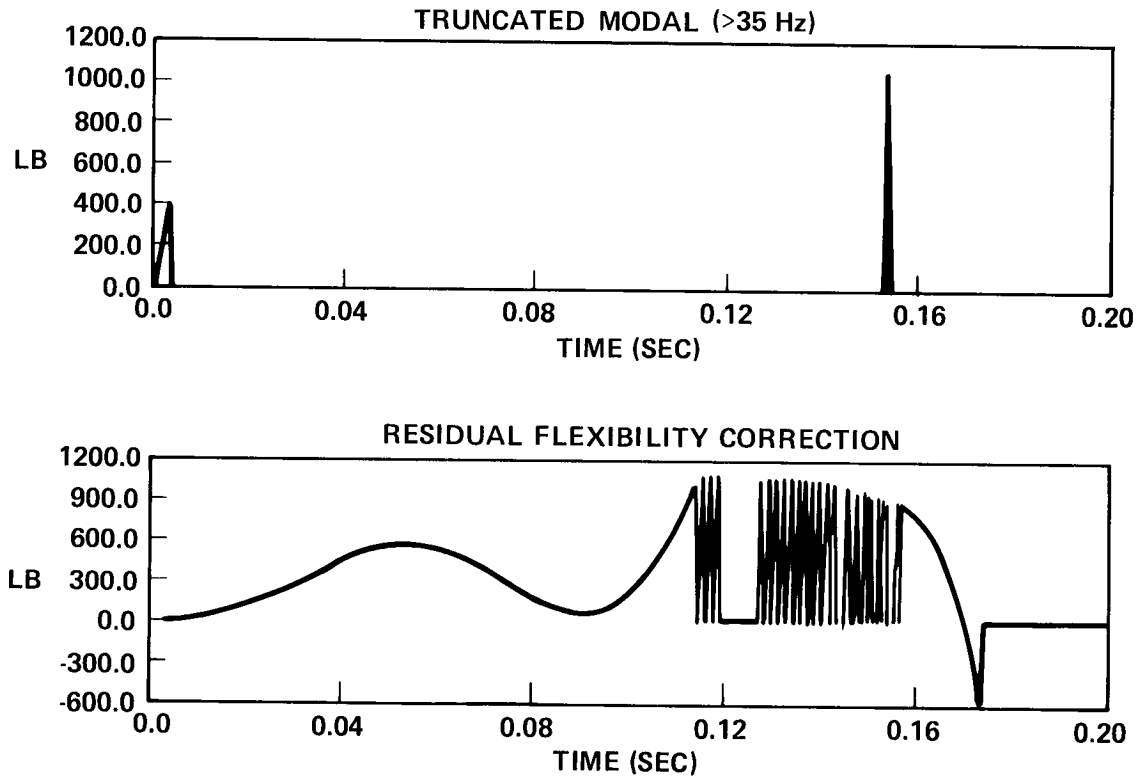

FIGURE 10. — STATIC FRICTION FORCES — RESIDUAL FLEXIBILITY VERSUS TRUNCATED MODAL

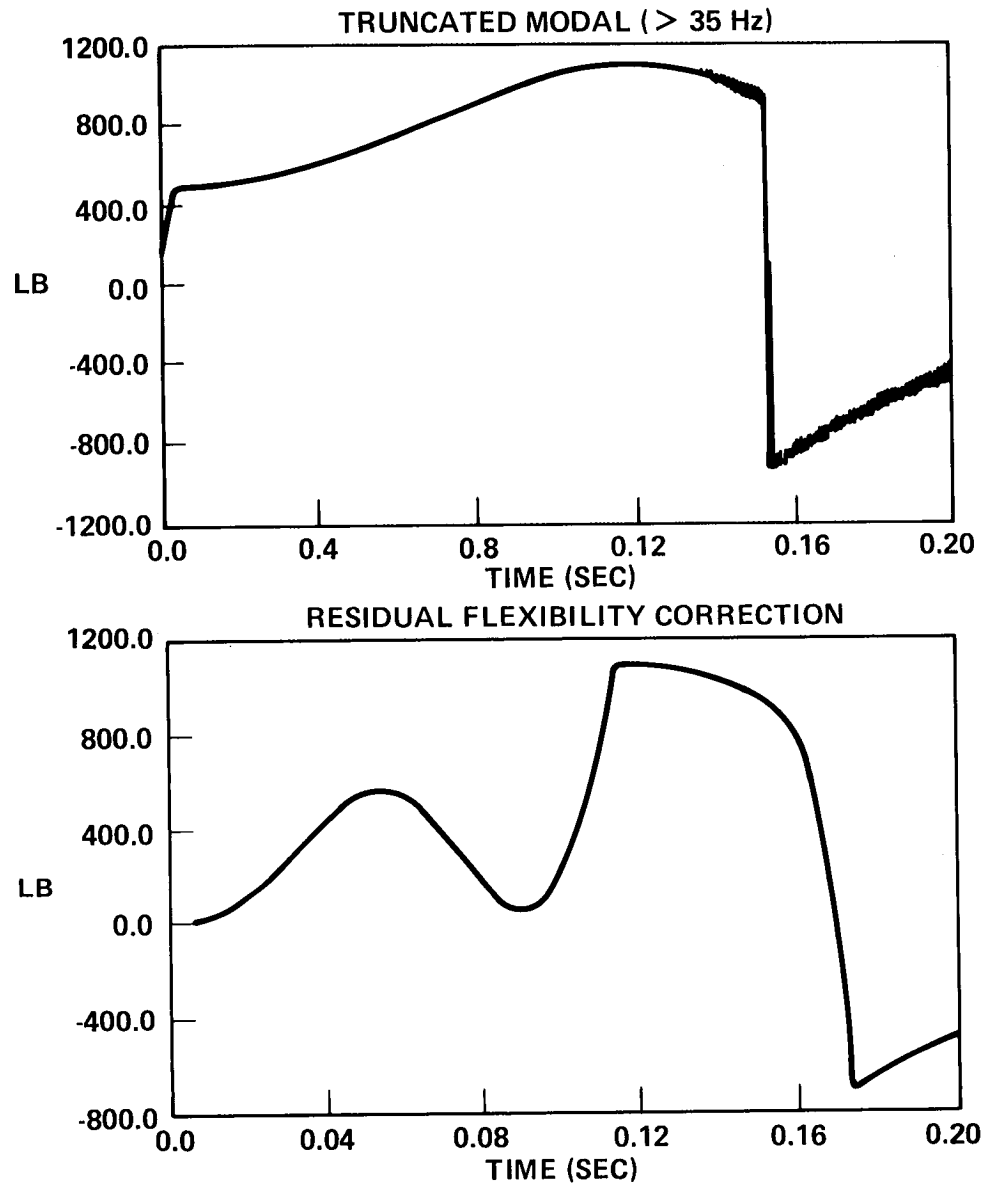

FIGURE 11. — TOTAL FRICTION FORCES — RESIDUAL FLEXIBILITY VERSUS TRUNCATED MODAL